JOURNAL OF PLANKTON RESEARCH | VOLUME 33 | NUMBER 11 | PAGES 1679–1695 | 2011

Response of *Euphausia pacifica* to small-scale shear in turbulent flow over a sill in a fjord

DEBBY IANSON[1]*, SUSAN E. ALLEN[2], DAVID L. MACKAS[1], MARK V. TREVORROW[3] AND MARK C. BENFIELD[4]

[1]FISHERIES AND OCEANS CANADA, INSTITUTE OF OCEAN SCIENCES, PO BOX 6000, SIDNEY, BC, CANADA V8L 4B2, [2]DEPARTMENT OF EARTH AND OCEAN SCIENCES, UNIVERSITY OF BRITISH COLUMBIA, 6339 STORES RD., VANCOUVER, BC, CANADA V6T 1Z4, [3]DEFENCE RESEARCH AND DEVELOPMENT CANADA ATLANTIC, PO BOX 1012, DARTMOUTH, NS, CANADA B2Y 3Z7 AND [4]DEPARTMENT OF OCEANOGRAPHY & COASTAL SCIENCES LOUISIANA STATE UNIVERSITY, BATON ROUGE, LA 70803, USA

*CORRESPONDING AUTHOR: debby.ianson@dfo-mpo.gc.ca

Received May 6, 2011; accepted in principle July 5, 2011; accepted for publication July 10, 2011

Corresponding editor: Mark J. Gibbons

Zooplankton in the ocean respond to visual and hydro-mechanical cues such as small-scale shear in turbulent flow. In addition, they form strong aggregations where currents intersect sloping bottoms. Strong and predictable tidal currents over a sill in Knight Inlet, Canada, make it an ideal location to investigate biological behaviour in turbulent cross-isobath flow. We examine acoustic data (38, 120 and 200 kHz) collected there during the daylight hours, when the dominant zooplankters, *Euphausia pacifica* have descended into low light levels at ~90 m. As expected, these data reveal strong aggregations at the sill. However, they occur consistently 10–20 m below the preferred light depth of the animals. We have constructed a simple model of the flow to investigate this phenomenon. Tracks of individual animals are traced in the flow and a variety of zooplankton behaviours tested. Our results indicate that the euphausiids must actively swim downward when they encounter the bottom boundary layer (bbl) to reproduce the observed downward shift in aggregation patterns. We suggest that this behaviour is cued by the small-scale shear in the bbl. Furthermore, this behaviour is likely to enhance aggregations found in strong flows at sills and on continental shelves.

KEYWORDS: euphausiids; zooplankton behaviour; turbulence; velocity shear; aggregation

INTRODUCTION

Zooplankton in the ocean are often observed to be patchy spatially (Yamazaki *et al.*, 2003). These aggregations occur for a variety of reasons; e.g. in response to a food source, as a social behaviour, to maintain position in convergent currents or to avoid predation (Mackas *et al.*, 1985; Genin, 2004). The presence of turbulence may also influence aggregation (e.g. Mackas *et al.*, 1993; Franks, 2001; Tsurumi *et al.*, 2005).

It has been theorized that turbulence (over spatial scales much larger than zooplankton) will enhance encounter rates of predators and prey (Rothschild and Osborn, 1988). Therefore, it may be expected that predators would be attracted to regions of higher turbulence or that prey may try to avoid such regions (which

doi:10.1093/plankt/fbr074, available online at www.plankt.oxfordjournals.org. Advance Access publication September 4, 2011

may also cause aggregations, e.g. Franks, 2001). It is also possible that animals may avoid turbulence because they find the velocity shear uncomfortable or because when the turbulence is strong enough, they may not be able to control their motion (e.g. Yen *et al.*, 2008) or it may impact their ability to feed (e.g. Tsurumi *et al.*, 2005). However, it is not yet possible to make broad generalizations on this topic. For example, at one time and location, certain species of copepods have been observed in the turbulent layer, presumably to feed, while others aggregated below this layer. It was suggested that the animals found below may have been avoiding turbulence (Mackas *et al.*, 1993). Similarly, evidence of both higher and lower feeding success in larval fish at elevated levels of turbulence has been found (Dower *et al.*, 1988; Mackenzie *et al.*, 1994, respectively).

Many species of zooplankton migrate vertically to low light environments during the day so that predators cannot see them (Banse, 1964). However, zooplankton have been found to migrate upward to depths where predators are absent, in the opposite direction to what one would expect if they were simply avoiding light (e.g. Ohman, 1990). Thus, some animals alter their behaviour in the presence of predators, likely due to hydromechanical (small-scale turbulent), visual or chemical cues (e.g. Onsrud *et al.*, 2004). In the case of small-scale turbulence, many zooplankters can sense and avoid velocity gradients due to fluid motion caused by their predators (Kiørboe *et al.*, 1999). This flight response is thought to be generally 'away from the turbulence', but not in a specific direction relative to a light gradient (i.e. up or down). However, Thomson and Allen (Thomson and Allen, 2000) observed acoustic patterns at mid-depths (between $\sim$50–200 m) near the continental shelf break, which suggested that euphausiids swam rapidly downward when larger predators were present during their daily pre-dawn descent, presumably as a response to one of the aforementioned cues. In this study, we explore the response of a specific zooplankter, *Euphausia pacifica*, to small-scale velocity shear in a larger-scale turbulent flow.

Euphausia pacifica is a large zooplankter ($\sim$1–2 cm) and is generally abundant in temperate coastal Pacific regions (Brinton, 1962). They have large eyes that are extremely sensitive to light (Mauchline, 1980). They use their vision to maintain position within low light intensities and undertake diel migrations on the order of 100 m (Boden and Kampa, 1965). Euphausiids lack a specialized gravity-direction sensor (e.g. statocysts in larger decapod crustaceans) but can detect 'down' via light gradients, or potentially by feeling differential drag and rotation on their bodies if they stop swimming and sink in calm water (in a similar manner to the copepods studied by Strickler, 1982). They are sensitive to small-scale fluid motions (e.g. Patria and Wiese, 2004) and may sense small-scale shear more effectively than the copepods studied by Kiørboe *et al.* (Kiørboe *et al.*, 1999) because they are larger and have additional sensory appendages.

Large aggregations of euphausiids have been observed along steep bathymetric slopes during upwelling (e.g. Simard *et al.*, 1986; Mackas *et al.*, 1997; Simard and Lavoie, 1999). Because these aggregations form and disperse daily, they must be caused by a rapid localized convergence of individuals rather than by changes in population size. Upwelling causes intermediate depth water, where these animals reside during the daylight hours, to be advected onshore where they encounter steep bathymetry and flows upward (e.g. in eastern boundary currents, Lentz, 1992). Simard *et al.* (Simard *et al.*, 1986) and Simard and Mackas (Simard and Mackas, 1989) hypothesized that euphausiids travelling passively in this current will seek to maintain their preferred light level and swim downwards when the flow develops a vertical component. As a result, aggregations form along bathymetric slopes at or slightly above the preferred light depth of the animals. In this research, we also observed aggregations of euphausiids at a sloping bottom, but not at their preferred light depth.

In our study, the sloping bottom is the inner sill in Knight Inlet. The tidal flow over this sill is predictable and strong, and has been well-studied, making it an ideal natural laboratory. We have constructed a simple physical model of the upstream flow based on models and observation (Farmer and Armi, 1999; Cummins, 2000). Zooplankton were modelled as behaviour-capable particles embedded in this flow during the daytime, after the animals have migrated down. Their resulting paths were traced and their abundances sampled as a function of location. We experimented by implementing various animal behaviours to see which ones were capable of producing spatial patterns that reconcile with acoustic data collected at the sill.

METHOD

Study site

Knight Inlet is a long (120 km), steep-sided, deep (>500 m) fjord in mainland British Columbia, Canada (Fig. 1). It has strong stratification primarily due to salinity (Baker and Pond, 1995). Winds are predominately along the fjord but because of the stratification, their effect is constrained to the upper 15 m (Baker and Pond, 1995). Our data were collected near and over the inner

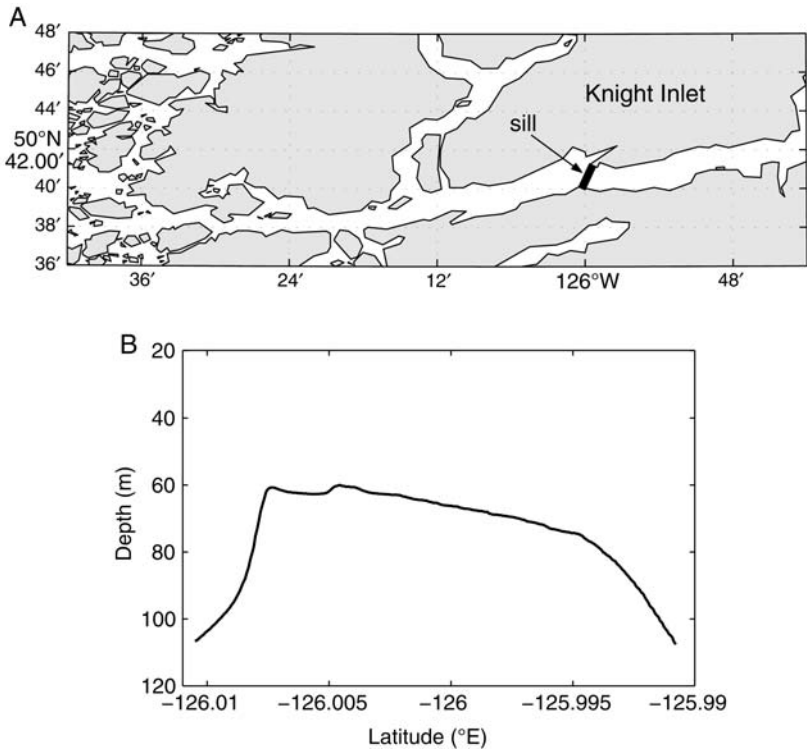

Fig. 1. (**A**) A map of Knight Inlet with the approximate location of the sill marked and (**B**) a longitudinal cross-section of the Knight Inlet sill, travelling from the seaward side, left to right at a constant latitude of 50.674°N, over a distance of 1.4 km, extracted from the echo-sounder data.

sill (~60 m deep) roughly midway up the inlet (Fig. 1). The sill bottom is rocky, with rocks ranging in size from cobble to boulders to bedrock (Tunnicliffe and Syvistski, 1983). Tidal amplitudes are about 3–4 m, so a large volume of water is exchanged diurnally (Baker and Pond, 1995) resulting in powerful tidal currents over the sill (consistently $>60\,\mathrm{cm\,s^{-1}}$ near the sea-surface, Cummins, 2000) and often creating an internal hydraulic jump on the downstream side at full flow (Klymak and Gregg, 2001). Turbulence levels, measured as dissipation, ϵ, in the strong surface flow are high, in the range of 10^{-5}–$10^{-4}\,\mathrm{W\,kg^{-1}}$ (Klymak and Gregg, 2004).

The sill is typical in shape relative to other sills formed by glaciers. It is not symmetric, rather it slopes more gradually on the landward (east) side of the sill (Fig. 1B) and attains a greater depth relative to the seaward side. There have been times during summer when asymmetry in flow over the sill during the latter part of the tide has been observed (Klymak and Gregg, 2004). However, the upstream flow is similar on both sides of the sill during the initial phase of both the ebb and flood tide (Klymak and Gregg, 2004). This flow is stratified and weakly turbulent ($\epsilon = 10^{-8}$–$10^{-7}\,\mathrm{W\,kg^{-1}}$) above the bottom boundary layer (bbl). Within the bbl (~5–10 m above the bottom), the flow is significantly more turbulent ($\epsilon = 10^{-7}$–$10^{-6}\,\mathrm{W\,kg^{-1}}$), consistent with the observations of Perlin *et al.* (Perlin *et al.*, 2005) who show that turbulence in a shelf bbl is more than an order of magnitude stronger than in the flow above and bbl measurements made at similar current speeds in the nearby coastal ocean (Dewey and Crawford, 1988). This flow has strong horizontal velocity shear and fluid properties are fully mixed.

Field collection

Intensive plankton surveys were undertaken aboard the CCGS Vector in November 2002 in the vicinity of the Knight Inlet sill (Fig. 1). The cruise was 2 weeks in duration and occupied several locations in the inlet (Trevorrow *et al.*, 2005). Data were collected over the sill during 4 days (17–18 and 22–23 November). Two-layer estuarine circulation (Hansen and Rattray, 1966) is low during autumn. Winds were weak to moderate during our cruises and the stratification in the fjord prevents their influence from penetrating below the upper 10–20 m (Baker and Pond, 1995). Thus, we were able to assume that tides dominated the physical circulation in our region of interest (60–100 m).

A three-frequency (38, 120 and 200 kHz) echo-sounder system was used to map the spatial distributions of the most abundant large zooplankton, namely

euphausiids, amphipods and siphonophores (Trevorrow *et al.*, 2005). The different frequencies were used to distinguish different biological target populations (Trevorrow *et al.*, 2005). For example, zooplankton such as *Euphausia pacifica* exhibit an increasing acoustic target strength with frequency (the 38 kHz signal is much weaker), whereas larger animals such as fish have a roughly constant acoustic target strength across these three frequencies. Surveys were repeated across the sill between the 100 m isobath on the eastern side of the sill and ~150 m isobath on the western side over a distance of about 2.3 km during day and night. (Figure 1B shows the bathymetry for a typical transect.) In this research, the focus is on euphausiid behaviour in turbulence, so we studied the acoustic data collected during daylight within a few kilometres of the sill, on the tidal-upstream side. At night, the euphausiid scattering layer had migrated upward into the upper 0–20 m of the water column, resulting in a loss of interaction with the deeper flow patterns, in which turbulence is predictable.

In addition to acoustic sampling, a variety of data were collected including a multiple net zooplankton sampler equipped with conductivity–temperature–depth and turbidity sensors (BIONESS, Bedford Institute of Oceanography Net Environmental Sampling System, Sameoto *et al.*, 1980), and *in situ* imaging (ZOOVIS, Zooplankton Visualization System, Benfield *et al.*, 2004). These data were used to 'sea-truth', or characterize taxonomic composition and target abundance in scattering layers. This sea-truthing was done primarily using BIONESS net tows because the acoustic and BIONESS sample volumes were comparable (Trevorrow *et al.*, 2005). The ZOOVIS samples were used only for comparison with the acoustic-derived abundance as its sample volume was low (about $10^4\times$ lower than either BIONESS or acoustic). Trevorrow *et al.* (Trevorrow *et al.*, 2005) provide further detail on acoustic sampling methods and sea-truthing. The acoustic data were then converted into individual abundances in spatial bins of 0.95 m (vertical) by 12 m (horizontal) (Appendix 1).

Data analysis

Every ~6–7 h, the current over the sill changes direction with the tide. We investigated the aggregation patterns in the acoustically derived animal abundances upstream of the sill on both the west and east side, depending on the tide. (In this study 'upstream' and 'downstream' always refer to the tidal current.) During daylight hours, the euphausiid scattering layer formed a narrow horizontal band at 60–90 m depth throughout the Inlet (Trevorrow *et al.*, 2005). Figure 2 shows a typical transect in the upstream flow, west-side in this case, collected at 11:19 local time at about peak flow (almost 3 h past slack tide). The transect provides us with the equivalent of a snapshot in time, showing animals travelling towards the sill over the slope and an aggregation already present at the sill. We presume that animals in the aggregation have been carried there earlier in the tide.

In Fig. 2, the incoming scattering layer is seen at 90 m depth, ~0.5–2 km from the sill (Fig. 2, $x \sim 800$–1200 m). The depth of the layer varied with transect, as expected, with isolumes changing depth depending on the light intensity and clarity of the water (e.g. Franks and Widder, 2002). We call this depth their "preferred light depth", $\bar{z}_i$. Although we were unable to measure light levels as low as those found at $\bar{z}_i$, we assume that light intensities were around 10^{-4} μW cm^{-2} between wavelengths 475 and 480 μm (Boden and Kampa, 1965; Widder and Frank, 2001). However, once the animals reached the sill, they consistently aggregated below $\bar{z}_i$ (Fig. 2).

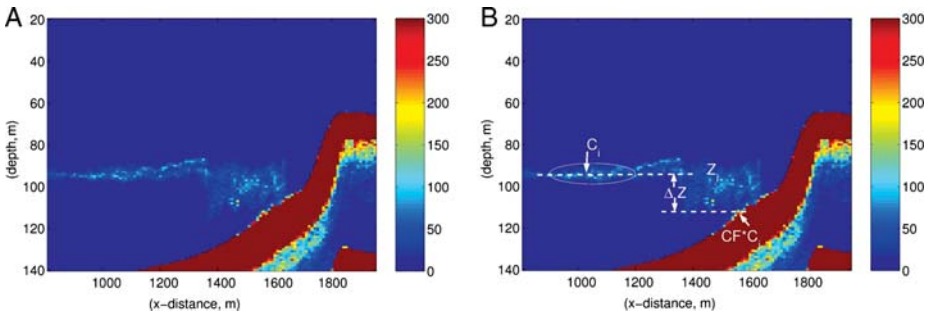

Fig. 2. (**A**) A typical pattern of *Euphausia pacifica* abundance (individuals m^{-3}) near peak flow. The current is travelling from left to right (eastward in this case). The seafloor is dark red (corresponding to abundance greater than 300 m^{-3}). Animals aggregate spread along the seabed in the bottom boundary layer below their preferred light depth. (**B**) The same transect of euphausiid abundance with data metrics; C_i, the incoming concentration; $\bar{z}_i$, the preferred light depth and $\Delta\bar{z}$, the displacement depth of aggregation, indicated.

Several metrics were developed to quantitatively describe this aggregation and allow comparison with model results. The concentration factor, CF, is defined as the ratio of the concentration of animals in the aggregation to the average concentration of animals that are upstream of the sill at the preferred light depth, C_i (from roughly 1 km upstream to the point where the sill depth is about 140 m, see Fig. 2B). The difference between the (average) preferred light depth, $\bar{z}_i$, and the depth of aggregation is Δz (Fig. 2B). The fact that the animals occupy such a narrow vertical range ($\bar{z}_i$) during the day allows the Δz to be observable. During the night when the animals are near the sea surface, they occupy a broader depth range and they may begin to descend slowly even when it is still dark (Thomson and Allen, 2000), making it much more difficult to determine a response (such as Δz) to potential turbulence. (There are also additional sources of backscatter near the sea surface, making data interpretation more complex, e.g. Ross *et al.*, 2007.)

These metrics were estimated from the abundance transects using a simple algorithm (see Supplementary Material). The vertical zone containing the majority of the biomass within each horizontal column of binned abundances was determined. The average depth, weighted by animal abundance, within the vertical band was calculated (again within each horizontal column of data). In the region upstream of the sill, these depths were averaged to yield $\bar{z}_i$. Similarly, the animal weighted depths were averaged within the aggregation that occurred at the sill to estimate Δz (by difference with $\bar{z}_i$, Supplementary Material).

Relationships between these metrics and phase of the semi-diurnal tide (φ), time of day and side of sill were investigated to support our modelling exercise. Two tidal indices were used as rough indicators of the flow throughout the water column over the sill, the current index (VI*)* represents flow velocity and flow index (FI) represents the cumulative flow (from the turn of the current tide):

$$\mathrm{VI} = \frac{A}{2} \sin\varphi \tag{1}$$

$$\mathrm{FI} = \frac{A}{2}(1 - \cos\varphi) \tag{2}$$

where A is the amplitude of the tide (specifically the absolute value of the difference between tidal heights at the sill at slack tides straddling the sampling period, ranging from 2.8 to 4.5 m in our data) and φ (radians) is defined by the time that the aggregation was sampled relative to the previous slack tide. (One cycle, 2π radians, is a complete tidal cycle, e.g. from one high tide until the next high tide.) These indices assume sinusoidal variation in tidal velocity that is locally uniform in the vertical (barotropic) and they do not attempt to account for the complex baroclinic flow that may develop even in the upstream current at the Knight Inlet sill (e.g. Klymak and Gregg, 2001). All parameters and symbols used are listed in Appendix 2.

Model

We use a model to test different zooplankton behaviours and attempt to reproduce the patterns in the data described above. The model allows us to control experiments and sample zooplankton concentration at any time and location; something that is not possible in the field. It is also possible to trace the paths of individual animals.

The flow in Knight Inlet is predictable and has been well studied. Thus, we implement a simple flow and turbulence pattern upstream of the sill (see Physical Model section). Individual particles (simulated zooplankters) are tracked in this flow using a Monte Carlo technique (e.g. Press *et al.*, 1992). A large number (576×10^6) of zooplankters are followed individually in the flow field. The zooplankton are released steadily over 4 h (40 000 every second). Each zooplankter enters the flow field over the deep plain, where the flow is not affected by the slope so there is no mean vertical velocity [1 km $\pm$ 25 m (random) upstream of the point where the sill slope begins]. They enter at a random depth between 90 and 100 m, the observed depth of the upstream scattering layer. The motion of the zooplankters is solved using a fifth order Runge–Kutta scheme (Press *et al.*, 1992) with an adaptive time step, which in our model ranges from 2×10^{-4} to 10 s. The final positions are binned (25 m horizontal and 0.5 m vertical bins) and that field is then contoured.

There are three distinct influences on a zooplankters path: (1) advection by the mean flow field (2) random motion by the turbulent flow field and (3) swimming motion of the zooplankter itself. Each influence is described in detail.

Physical model

The mean flow field (influence 1) is a simple, steady, two-dimensional representation of the modelled flow of Cummins (Cummins, 2000) upstream of the Knight Inlet sill (Fig. 3). This model was validated by the observations of Farmer and Armi (Farmer and Armi, 1999). The bbl thickness, z_b (shaded, Fig. 3) was specified as 10 m. The lower portion of this layer, the part that flows right along the seafloor, is termed the 'surface' layer, z_{sl}. (In this paper 'surface'

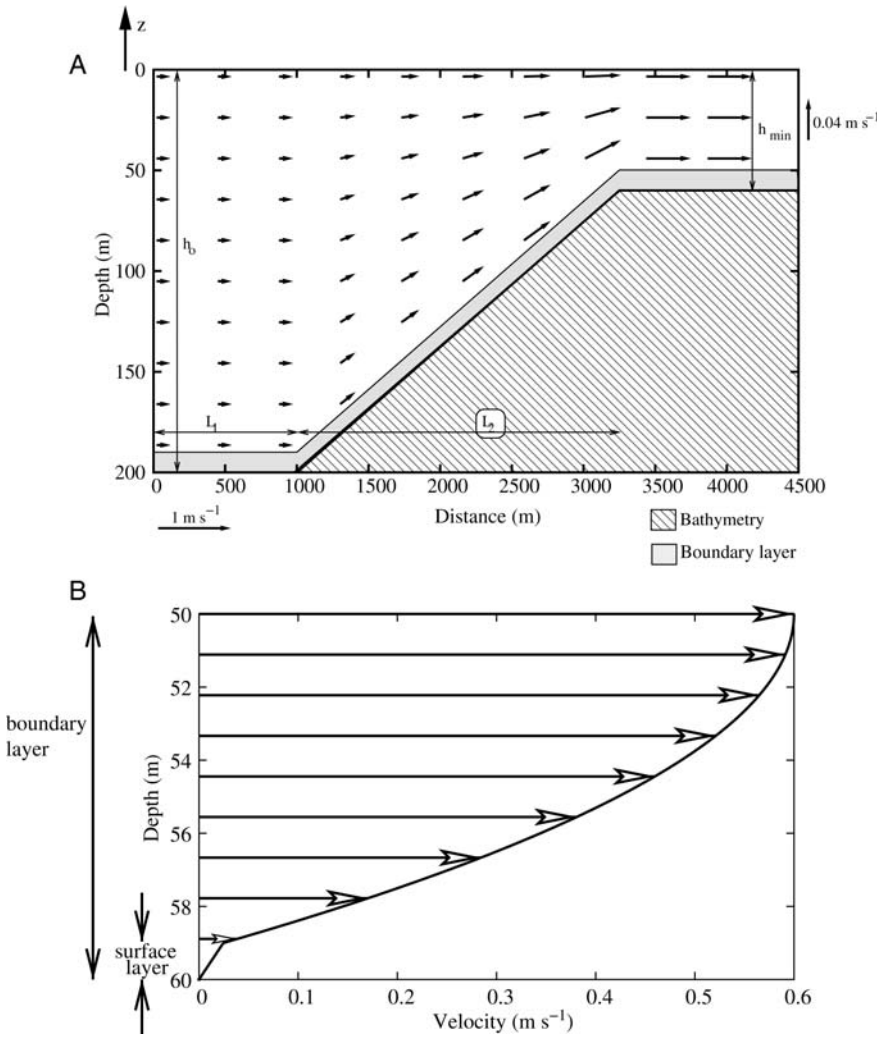

Fig. 3. (**A**) Bathymetry of model ridge on the eastward side of the sill [see equation (3)]. The mean flow field above the boundary layer is shown. Velocity scale vectors are shown. The vertical and horizontal scales are different. The bottom boundary layer, 10 m above the bottom, is shaded. (**B**) Depth profile of the mean boundary layer flow at the sill between 50 and 60 m. The bottom 1 m of the boundary layer is the 'surface' layer.

will always refer to the seafloor–fluid interface, rather than the air–sea interface.) The thickness of this surface layer is 10% of z_b (Stull, 1988). Details of the topography and the mean flow in and above the bbl are given in Appendix 3. All parameters and symbols used are listed in Appendix 2.

Turbulence (influence 2) causes groups of animals to disperse. It is modelled as a diffusive process on scales set by the eddy viscosity, $\mathcal{D}$. In our model, each zooplankter makes a random walk in two dimensions (x and z) after each time step. This random walk is dependent on the value of $\mathcal{D}$ and the time step, Δt. Details of the values used for the eddy viscosity and the corrections to simple random walk required by the variation in the eddy viscosity (in the bbl) are given in Appendix 3.

Zooplankton behaviour

We experimented with various zooplankton swimming behaviours (influence 3) for both east and west sill geometries (Table I). We started with the most basic; the null case, or no response (1) and then built in complexity until results similar to the observations were obtained.

In each model scenario, the animals avoid the bottom, as *Euphausia pacifica* have been observed to in nature (D.L.M. and M. Tsurumi, Vancouver, using a remotely operated vehicle and W. Hamner, Los Angeles, personal communication). When they come within 1 m of the bottom, they swim up until they are cued to swim down again by turbulent shear or light level (depending on experiment).

Table I: Zooplankton behaviour model experiments

Model run	Description
Animals respond only to light levels, i.e. depth (exp. 1–3)	
1. No swimming	Passive tracer—null experiment
2. Maintain depth	At maximum swim velocity, $zoo_{max} = 10$ cm s^{-1} (Genin *et al.*, 2005)
3. Maintain depth	Swim velocity increasing with depth away from z_i, limited by zoo_{max}; $w_{zoo} = zoo_{basic}\frac{z - z_i}{z_{tot}}$ where zoo_{basic} is a comfortable euphausiid swim velocity (De Robertis *et al.*, 2003) and z_{tol} is 5 m
In addition to depth, animals respond to the bbl, i.e. small scale shear (exp. 4–8)	
4. Freeze and sink	Euphausiids sink at 0.5 cm s^{-1} (based on Rubjakov, 1970)
5. Escape response	Euphausiids swim in random direction at zoo_{max}
6. Swim down	Euphausiids swim downward at zoo_{max}
7. Swim down	Euphausiids swim downward at zoo_{max}, and when close to the bottom (within 5 m) they swim down along, and parallel to, the bottom
8. Swim down	As exp. 7 except they only are able to swim for 5 min at zoo_{max}; after which they become exhausted and swim at zoo_{basic}

All parameters are listed in Appendix 2.

RESULTS

Analysis of acoustic observations

The aggregations at the sill were consistent in their general pattern (Fig. 2A). On the tidal upstream side of the sill (whether east or west, depending on the tidal phase), the zooplankton scattering layer tended to dip 10–20 m below the preferred light depth (z_i) as the sill was approached (Table II). The strongest aggregation was found in a dense layer oriented along and immediately above the seabed (Fig. 2A). Animals were concentrated in these aggregations by factors ranging from 2 to 30 (relative to C_i), more often in the lower end of this range (Table II; mechanisms responsible for this concentration are discussed with the model results). Of the 10 transects, 3 were collected on the east side of the sill and 7 from the west side. The west (seaward) side of the sill consistently had higher concentrations of euphausiids by a factor of roughly 2–4 relative to the east (fjord side) when comparing data collected on the same day. Data collected on the same tide (upstream) indicate that estimations of Δz were robust (varying only by 1 and 3 m on the westward side and 6 m on the eastward side, Table II). The concentration factor was more variable (varying by as much as a factor of 2, Table II).

There are not enough data available to be conclusive about possible patterns in Δz. In general Δz is similar on both sides of the sill and not related to tidal indices [equations (1) and (2)]. As expected, CF appears to increase as the tide progresses and more animals are brought into the aggregation, i.e. with the proxy for integrated flow [equation (2); Table II]. This increase is apparent on both sides of the sill (with the exception of data collected 17th November on the west side shortly after the turn of the tide, that has fewer animals, especially in the incoming scattering layer, $\sim 5\times$ less relative to other transects). CF shows no relation to current index, implying that the animals are able to overcome the range of vertical velocities that they experience (Table II).

In the absence of hydrodynamic disturbance, we expect the preferred depth of incoming animals to be related primarily to *in situ* light intensity. However, time of day is not a sufficient indicator of light intensity. There does not appear to be a relationship between z_i and time of day, or incoming velocity, in our data. The depth of incoming animals, z_i ranged from 60 to 95 m, with a mean of about 85 m. In addition Δz did not appear to be related to time of day, or even z_i. We suggest that it is more likely that Δz is affected by the thickness of (and shear within) the bbl.

Model experiments

Each model experiment is discussed in the context of the observations and the data metrics described above.

Passive particles (1)

A truly passive particle, or a non-swimming zooplankter, will be carried with the flow. They rise smoothly from their preferred depth (90–100 m) and cross the sill well above (27.6–30.5 m) the bbl (Fig. 4A). A passive particle experiences all components of the flow. Thus, a group of such particles has the same divergence/convergence properties as the flow above the bbl: none. There is no aggregation or concentration of such particles.

Depth maintaining behaviour (2) and (3)

Zooplankton have been observed to swim vertically to maintain their preferred depth ($z_i = 90$–100 m in this case). As the flow starts over the slope and acquires a vertical velocity, the euphausiids can easily swim downward, against the vertical component of the flow, and maintain their depth (Fig. 4B). This behaviour was modelled in two ways, experiments (2) and (3) (Table I). The results of both experiments are similar. Even swimming more slowly (exp. 3), the animals are able to overcome the vertical component of the current and so aggregate at the

Table II: Table of data metrics determined from acoustic abundances (see Data Analysis)

Date, day month	Time, local	Z_i (m)	ΔZ (m)	CF–	φ (rad)	t_a (hrs)	VI (m)[a]	FI (m)
West side of sill (seaward)								
17 November	11:24	88	21	26	0.169	0:21	0.34	0.028
18 November	10:41	94	13	30	2.699	5:22	0.71	3.1
18 November	10:41	97	16	20	3.041	6:03	0.17	3.3
23 November	10:14	94	8.8	2.8	1.073	2:03	1.2	0.73
23 November	10:57	93	9.2	5.3	1.424	2:43	1.4	1.2
23 November	11:19	93	8.5	3.5	1.529	2:55	1.4	1.3
23 November	11:19	93	8.5	6.8	1.623	3:06	1.4	1.5
East side of sill (landward)								
17 November	14:52	60	19	21	1.716	3:33	1.9	2.3
17 November	14:52	58	13	8.6	2.006	3:45	1.8	2.8
22 November	14:54	80	20	1.9	0.525	1:10	1.1	0.3

The time listed is the start time of the transect, while φ and t_a are calculated at the time the aggregation was sampled relative to the previous slack tide. (Since we only study the upstream phase of the tide φ ranges from 0 to π.) Some transects are from the same tide and at times there is more than one pass over the sill in the same transect (listed as separate data, but with the same start times). Two significant figures are reported for data metrics.

[a]The velocity index is proportional to the flow velocity although it has units of length.

sill roughly at their preferred light depth (Fig. 4B). The analysis yields a small $\Delta\mathcal{Z}$ of −0.8 m (i.e. 0.8 m above their incoming depth) (Table III). The absolute error in our method for determining model $\Delta\mathcal{Z}$ (Supplementary material) is about 0.2 m.

Aggregation mechanisms. These zooplankton are passive in the horizontal and thus have the same divergence/convergence properties as the horizontal flow. The horizontal velocity (u_a) increases as the flow enters the region over the slope coming from the deep plain. Thus, there is a weak zooplankton divergence (they become more spread out in the horizontal) over the slope (Fig. 4B, $x \sim 2000-2500$ m) followed by a strong convergence where the layer encounters the slope of the sill and zooplankton swim downwards to maintain their depth (Fig. 4B, $x \sim 2600-2800$ m).

To quantify the aggregation processes, consider first an imaginary scenario with a simplified flow such that the mean flow is constant over the ridge (implies large depth) and does not slow down in the bbl but is turbulent. The zooplankton will be carried up the slope by the mean flow and spread through part of the bbl by the turbulence. The net effect is to take an initial biomass layer thickness, L, of say 10 m and concentrate it into a thinner layer, ℓ, over the slope. This type of convergence, first identified over the continental slope (Mackas *et al.*, 1997) and canyons (Allen *et al.*, 2001), is given by L/ℓ, where ℓ is dependent on the properties of the turbulent flow in the bbl and on the behaviour of zooplankton when they can see the bottom. We have assumed that they stop trying to maintain their depth and swim upward once they reach the surface layer (the base of the bbl, just above the sea floor) so the final thickness is about 1.5 m. Thus, we would expect a concentration factor of about 6 or 7; the simulation gives 5.

Now consider the more realistic flow such that the mean flow increases over the topography and goes to zero against the slope. In this case, the zooplankton are further concentrated because they are choosing to swim downward across the vertical gradient of horizontal flow into slower moving water. The net result of the two effects is a concentration increase by a factor of

$$\frac{L}{\ell}\frac{V_i}{V_b}$$

where V_i is the initial horizontal velocity of the flow and V_b is the flow in the bbl (average velocity experienced by the zooplankton). If the incoming flow velocity is 0.36 m s^{-1} (in water of 100 m depth), then the velocity in the bbl at 2.0 m above bottom (at the convergence) is 0.09 m s^{-1}. Given sufficient time (>15 h in our case), the total enhancement (or CF) in the model is 34×.

Over a shorter time, such as an incoming tide, the theoretical concentration increase for the given geometry is approximately

$$\frac{V_i t s}{\ell}$$

where t is the total time elapsed after the first zooplankton reach the sill and s is the slope of the ridge. Running the model experiment for 4 h (the time for developed flow of one tide in our study area) yields a CF of about 22 on the landward side of the sill (in a 1 m thick layer) and 45 on the seaward side (in a 4.5 m thick layer). The theory above predicts a CF of 20 and 80, for landward and seaward geometries, respectively, if the animals have been flushed away from the sill during the previous tide.

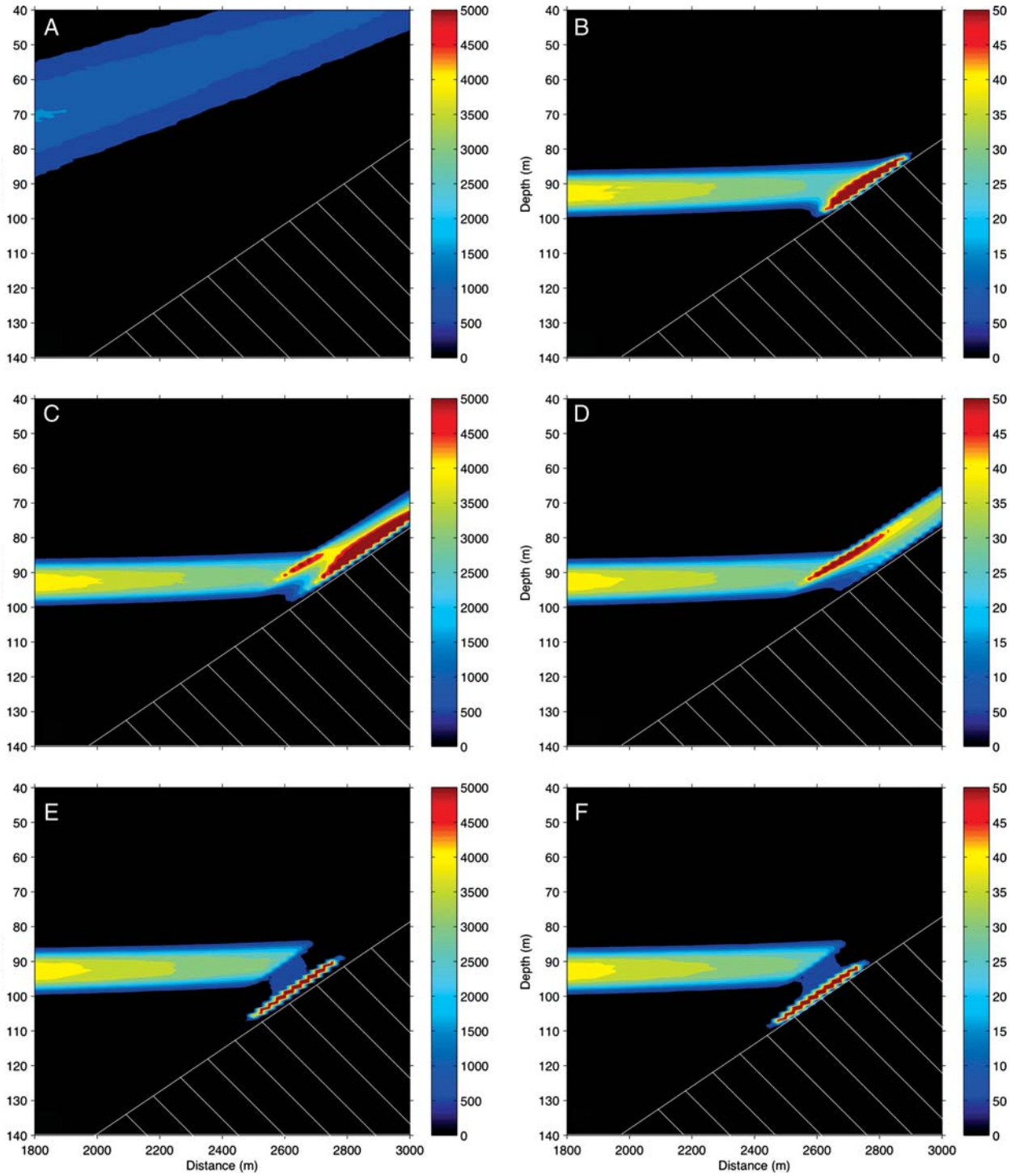

Fig. 4. Colour contour plots of modelled concentration. The sill is shown as the white cross-hatched region. Flow goes from left to right, landward side of sill. (**A**) Passive zooplankton (exp. 1); (**B**) zooplankton maintain depth and swim at their maximum swim velocity (exp. 2); (**C**) zooplankton maintain depth above the boundary, in the boundary layer they freeze and passively sink (exp. 4); (**D**) zooplankton maintain depth above the boundary layer, in the boundary layer they sprint in random directions (exp. 5); (**E**) zooplankton maintain depth above the boundary layer, in the boundary layer they swim downward at maximum velocity (exp. 6); (**F**) zooplankton maintain depth above the boundary layer, in the boundary layer they swim downward and near the bottom they alter their trajectory to be downward along the topography, again at maximum velocity (exp. 7).

Table III: ΔZ in the modelled responses for various experiments

Model run	Depth in	ΔZ
3 depth maintain	90.7 m	−0.8
4 freeze and sink	90.6 m	−11.8
5 swim away in all directions	91.0 m	−15.3
6 swim down	90.9 m	6.8
7 swim down and along (landward)	90.8 m	8.5
7 swim down and along (seaward)	84.3 m	13.3

A negative ΔZ refers to an upward displacement.

The assumption that the flow upslope in the bbl is negligible over the time of the aggregation is reasonable for a sill with a shallow slope, but is less appropriate as the slope becomes steeper, thus theoretical CF is overestimated on the seaward side.

The simple depth maintenance behaviour in the model reproduces the observed aggregation against the sill and enhancements in concentration of the same order as in the data (see Table II, CF). However, this model does not result in any downward movement ($\Delta\mathcal{Z}$) at the slope (Table III). The following experiments consider zooplankton behaviour in response to perceived turbulence.

Zooplankton freeze when they encounter boundary layer turbulence (4)

When model zooplankton 'freeze', or stop swimming, in response to turbulence, they sink at a rate of 0.5 cm s^{-1} (exp. 4). This sinking rate is not enough to overcome the upward flow velocities on either side of the sill for typical tidal currents at the Knight Sill and so animals are swept up and over the sill (Fig. 4C). They would have to sink significantly faster (>2 cm s^{-1}) to avoid this fate. They still converge near the sill prior to being swept away (Fig. 4C) but there is no drop, rather $\Delta\mathcal{Z}$ is about 12 m above their preferred light depth (Table III).

Zooplankton have an escape response and swim in random directions in response to turbulence (5)

If zooplankton swim randomly in all directions at their maximum speed, they are also carried over the sill (exp. 5, Fig. 4D). The abundance pattern is different than the sinking response above. There is less aggregation and more dispersion of the zooplankton and they travel faster. Similarly, they are displaced upward by roughly 15 m, rather than downward, at the sill (Table III).

Zooplankton sprint downward in response to boundary layer turbulence (6)

When the euphausiids escape response is to swim downward (as suggested by Thomson and Allen, 2000), the concentration patterns begin to produce a downward movement at the sill ($\Delta\mathcal{Z}$ ~7 m, Table III) and look more similar to the observations shown in Fig. 2A (Fig. 4E).

Zooplankton sprint downward and along the bottom in response to turbulence (7) and (8)

When the euphausiids do not only swim vertically but are also allowed a horizontal component so that they may swim down along the bottom of the sill (Fig. 4F), the aggregation shifts a little further down the slope ($\Delta\mathcal{Z}$ ~8–13 m, Table III). We assume that since they are not able to sense gravity when swimming, only light gradients, that they choose to swim further down while visually avoiding the bottom (see previous section). They swim rapidly for a limited time from the initial encounter with the bbl and slow when they are close to the bottom (see next section). Thus, including exhaustion in the swimming behaviour (exp. 8) has only a small effect on the aggregation at the ridge (not shown) relative to exp. 7 (Fig. 4F). The centroid and deep end of the aggregation are nearly identical but the shallow end of the aggregation is slightly extended in exp. 8. Of all the models tested, the distribution of zooplankton in these experiments (on both the landward and seaward side of the sill; Fig. 5) are the most similar to field observations (Fig. 2A, Table II).

On the steeper seaward side, we see a larger shift upward because the vertical (upward) flow velocities are higher over the sill (Fig. 5). We used steady flow for the model runs described here to increase model efficiency and because time-varying flow did not influence the results. The vertical displacement obtained in time-varying flow depends simply on the velocity just prior to the time of sampling (the velocity that animals in the aggregation experienced as they approached the bbl). At peak flow, the vertical (upward) flow velocity over the sill is highest, causing an upward shift in the simulated scattering layer (as in the landward case above), so $\Delta\mathcal{Z}$ is slightly smaller (about 1 m relative to $\Delta\mathcal{Z}$ at half flow).

Path of a zooplankter

To confirm the behaviour of individual zooplankters rather than the bulk properties of thousands, the paths of six animals are traced during the incoming tide for exp. 7 behaviour (Fig. 6). The zooplankton travel towards the sill moving up and down in the background

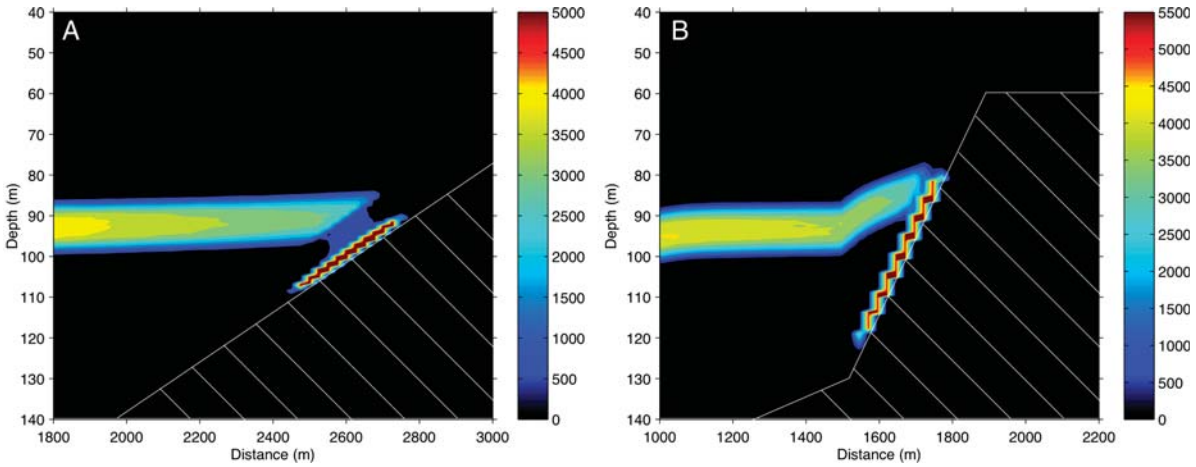

Fig. 5. Colour contour plots of modelled concentration. The sill is shown as the white cross-hatched region. Flow goes from left to right. (**A**) On the landward side of the sill zooplankton maintain depth above the boundary layer, in the boundary layer they swim downward, near the bottom they alter their trajectory to be downward along the topography. (**B**) Same as (A) but for the ridge bathymetry on the western or seaward side of the sill.

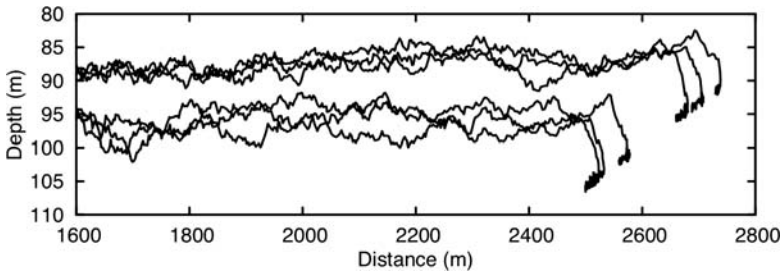

Fig. 6. Six tracks (bold traces) that illustrate depth maintenance above the boundary layer, downward swimming in the boundary layer that turns to parallel the slope as the slope is approached and upward swimming in the surface layer. Flow is left to right.

turbulence swimming gently to maintain their preferred depth range. Where the slope begins ($x = 1250$ m), the horizontal velocity increases and they are carried upwards in the current, but still swim to maintain their depth. When they reach the bbl, they swim swiftly downward toward the bottom. As they approach the sill bottom, they slow and their tracks turn to follow the topography down.

DISCUSSION

Animal behaviour is clearly more complex than our simple model representations. However, our results indicate that *Euphausia pacifica* must actively swim downward, or to a lower light environment, when they encounter the bbl and small-scale velocity shear. Turbulence levels in the bbl in our study area are expected to be moderately strong, 10^{-7}–10^{-6} W kg^{-1}. For comparison, *Euphausia pacifica* themselves are able to generate higher turbulence when they are found in dense schools, 10^{-5}–10^{-4} W kg^{-1} (Kunze *et al.*, 2006), while typical turbulence levels at depths below the wind mixed layer in the ocean are only about 10^{-9} W kg^{-1}.

Because these animals are found in such a narrow vertical range during daylight hours (*sensu* Birch *et al.*, 2009) and given the well-defined physical flow in our study area, we were able to observe this behaviour in the bbl. They may behave similarly throughout the water column, for example in response to shear caused by wind forcing or even by a predator. The predator-escape response has only been observed anecdotally thus far. However, it seems logical that rapid responses occur at times because so much of a euphausiid's body is devoted to sprint swimming (Verity and Smetacek, 1996). On the other hand, it appears that *Euphausia pacifica* do not respond visually to predators in this manner, at least when the fish are more than 20 cm away (De Robertis *et al.*, 2003). A downward response to turbulence caused by wind forcing in the upper mixed layer would be difficult to observe, but may be of consequence to ecological models of grazing by zooplankton.

Strong aggregations of zooplankton have been found at other sea slopes during the day where currents flow upwards and the animals are able to maintain their light depth (Genin, 2004). In eastern boundary currents, the cross-isobath, or upwelling, flow is relatively weak. The strong flow is in the along-isobath (along-shore) direction (Lentz, 1992). Given the weak flow, the documented aggregations in these regions (e.g. Simard and Mackas, 1989) are more dense than might be expected for diel migrators. However, the currents in the along-shore direction are strong and consistent enough to produce boundary layer shear even if the on-shore current is not. Our results suggest that the aggregations occurring at these locations may be further concentrated, in-line with observations, by the downward swimming behaviour that we describe, because travelling into slower moving water causes an additional convergence.

The euphausiids do not appear to be moving downward in response to predators. At times larger animals, presumably fish, are found in the bbl at the sill in dense aggregations (seen in the lower frequency, 38 kHz, data). However, these large scatterers were usually well below the euphausiids' preferred light depth (that ranged from 60 to 100 m) at around 140 m.

The motivation for the model study relies on the acoustic data. The conversion from acoustic backscatter to animal abundance, and especially to a specific zooplankter, is complex and requires many assumptions (e.g. Benfield *et al.*, 1998). We were fortunate to have high abundances in 2002 and *in situ* net samples to satisfy some of the important assumptions. For example, the net samples showed that a single species dominated the intense scattering layer (Fig. 2) and that its size distribution was Gaussian (Fig. 3, Trevorrow *et al.*, 2005). The 38 kHz data confirmed that the contribution of larger animals such as fish was minimal within the scattering layer and the abundance algorithm was designed to filter out that portion of the signal (Trevorrow *et al.*, 2005). In addition, the ZOOVIS data suggest that our acoustic abundances are underestimated by roughly a factor of 2 which could be a result of changes in swimming orientation (Trevorrow *et al.*, 2005). Thus, we caution the reader that our quantitative estimates from data should be allowed a margin of error. The primary function of this analysis (Table II) is to allow comparison between the data and model results.

The observations show the higher concentrations of animals at the sill that both physical theory and model predict. On the landward side, all three measures of this enhancement (CF) agree, at the high end of the range in the data (see Table II, and Model results). On the seaward side, model and theory over-predict CF (see Model results) relative to the data. The model is a factor of 1.5× higher than the high end of the data range (30, Table II) while the theoretical CF is even higher, almost double that of the model. We never observed CF higher than 30× in the data and consider that model and theory may allow overcrowding that does not occur in nature. The model also has the advantage of injecting many animals at consistent intervals so that clear and repeatable responses are possible. In the observations, we do not know how many animals have been swept toward the sill prior to the snap-shot that the transect provides.

Exploration of relationships between these metrics (CF and Δz) with current speed and integrated flow [or time in tidal cycle, see equations (1) and (2)] are inconclusive because there are not enough data. However, they do suggest that CF increases as the tidal cycle progresses and more animals are carried toward the sill as one would expect. The bbl may become thicker and more turbulent as the mean flow increases (lagging the mean flow) potentially influencing both Δz and CF. Model runs show that decreasing bbl thickness from 10 m, used in our standard model runs, to 5 m (after Cummins, 2000) led to a similar (approximately 50%) decrease in the downward shift of the aggregation, while CF was similar. Thus we might expect Δz to increase as the tidal cycle progresses.

We assume that the depth of isolumes remains constant in the region upstream of the sill. The fresher surface layer, which may absorb more light, becomes significantly thicker over the top of the sill. However, it is constant upstream of the sill, deepening slightly by ~10% in the region of aggregation (Klymak and Gregg, 2004). Regardless, if there were more light absorption above the aggregation, relative to the region upstream, then we would expect the euphausiids to be found higher in the water column to maintain their light depth, rather than lower, as the sill is approached.

The data are consistent on either side of the sill despite differences in slope and possibly in flow characteristics during the later part of the tide. On the west side, water around the preferred light depth ($z_i \sim$ 90 m) may slow as the tide progresses due to a dense (saltier than on the landward side) body of water often present there (observed during summer by Klymak and Gregg, 2003). More data were collected on the west side of the sill, and two of those transects (collected on 11/18, Table II) occur when the water at z_i at the sill may be moving slowly. In both cases, aggregations are seen below z_i. If the water is no longer turbulent, we do not know why *Euphausia pacifica* remain below their preferred light depth, unless there is a lag time before they venture back up after experiencing hydrodynamical disturbances.

CONCLUSIONS

We propose a new mechanism to enhance zooplankton aggregation and a downward swimming response to small-scale shear by zooplankton. Bio-physical aggregation in the marine environment in response to upwelling flow over topographical features has been observed and documented (Genin, 2004). Previous studies indicate that during the day, light-sensitive animals choose to maintain their light depth (Genin, 2004). However, in the strong tidal flows at the Knight Inlet sill *Euphausia pacifica* aggregate below this depth. We suggest that the downward shift in aggregation is caused by a behavioural response to small-scale velocity shear in the turbulent bbl. This response causes the concentration of the animals to be further enhanced as they move into even slower moving water. In addition, our model shows that animals must actively swim down to a lower light environment to produce a downward shift in concentration patterns in such a strong current. It is not possible to produce such a pattern by freezing and sinking or by swimming fast in random directions. We suggest that this response by euphausiids is not confined to our study area and that it is likely an evolved response to small-scale velocity shear (turbulence), caused by wind, tides or predators, throughout the water column.

SUPPLEMENTARY DATA

Supplementary data can be found online at http://plankt.oxfordjournals.org.

ACKNOWLEDGEMENTS

We thank the officers and the crew of the CCGS Vector. We are grateful to J. Klymak and P. Cummins for helpful conversations concerning the physical flow and to M. Tsurumi for her initial work on this project. We thank D. Tuele for help with the data processing and sampling; D. Yelland for assistance with the acoustic data; P. Chandler for providing bathymetric data; A. De Robertis for helpful correspondence concerning euphausiids and T. Kiørboe for his helpful comments on the manuscript.

FUNDING

This work was supported by the Office of Naval Research (N00014-01-1-0274, N00014-01-1-0273 and N0014-02-1-0012) (Program Manager J. Eckman) and the National Science and Engineering Research Council of Canada.

REFERENCES

Allen, S. E., Vindeirinho, C., Thomson, R. E. *et al*. (2001) Physical and biological processes over a submarine canyon during an upwelling event. *Can. J. Fish. Aquat. Sci.*, **58**, 671–684.

Baker, P. and Pond, S. (1995) The low-frequency residual circulation in Knight Inlet, *British Columbia. J. Phys. Oceanogr.*, **25**, 747–763.

Banse, K. (1964) On the vertical distribution of zooplankton in the sea. *Prog. Oceanogr.*, **2**, 53–125.

Benfield, M. C., Schwehm, C. J., Fredericks, R. G. *et al*. (2004) Measurement of zooplankton distributions with a high-resolution digital camera system. In Strutton, P. and Seuront, L. (eds), *Scales in Aquatic Ecology: Measurement, analysis and simulation*. CRC press, pp. 17–30.

Benfield, M. C., Wiebe, P. H., Stanton, T. K. *et al*. (1998) Estimating the spatial distribution of zooplankton biomass by combining video plankton recorder and single-frequency acoustic data. *Deep Sea Res. II*, **45**, 1175–1199.

Birch, D. A., Young, W. R. and Franks, P. J. S. (2009) Plankton layer profiles as determined by shearing, sinking, and swimming. *Limnol. Oceanogr.*, **54**, 397–399.

Boden, B. P. and Kampa, E. M. (1965) An aspect of euphausiid ecology revealed by echo- sounding in a fjord. *Crustaceana*, **9**, 155–173.

Brickman, D. and Smith, P. C. (2002) Lagrangian stochastic modeling in coastal oceanog- raphy. *J. Atmos. Oceanic Tech.*, **19**, 83–99.

Brinton, E. (1962) The distribution of Pacific euphausiids. *Bull. Scripps Inst. Oceanogr.*, **8**, 51–270.

Cummins, P. F. (2000) Stratified flow over topography: time-dependent comparisons between model solutions and observations. *Dyn. Atmos. Oceans*, **33**, 43–72.

De Robertis, A., Schell, A. and Jaffe, J. S. (2003) Acoustic observations of the swimming behavior of the euphausiid *Euphausia pacifica* Hansen. *ICES J. Mar. Sci.*, **60**, 885–898.

Dewey, R. K. and Crawford, W. R. (1988) Bottom stress estimates from vertical dissipation rate profiles on the continental shelf. *J. Phys. Oceanogr.*, **18**, 1167–1177.

Dower, J. F., Pepin, P. and Leggett, W. C. (1988) Enhanced gut fullness and an apparent shift in size selectivity by radiated shanny (*Ulvaria subbifurcata*) larvae in response to increased turbulence. *Can. J. Fish Aquat. Sci.*, **55**, 128–142.

Farmer, D. L. and Armi, L. (1999) Stratified flow over topography: the role of small scale entrainment and mixing in flow establishment. *Proc. Roy. Soc. Lond.*, **455A**, 3221–3258.

Foote, K., Everson, I., Watkins, J. *et al*. (1990) Target strengths of Antarctic krill (Euphasusia superba) at 38 and 120 kHz. *J. Acoust. Soc. Am.*, **87**, 16–24.

Franks, P. (2001) Turbulence avoidance: an alternative explanation of turbulence-enhanced ingestion rates in the field. *Limnol. Oceanogr.*, **46**, 959–963.

Franks, T. M. and Widder, E. A. (2002) Effects of a decrease in downwelling irradiance on the daytime vertical distribution

patterns of zooplankton and micronekton. *Mar. Biol.*, **140**, 1181–1193.

Genin, A. (2004) Bio-physical coupling in the formation of zooplankton and fish aggregations over abrupt topographies. *J. Mar. Syst.*, **50**, 3–20.

Genin, A., Jaffe, J. S., Reef, R. *et al.* (2005) Swimming against the flow: a mechanism of zooplankton aggregation. *Science*, **308**, 860–862.

Hansen, D. V. and Rattray, M. J. (1966) New dimension in estuary classification. *Limnol. Oceanogr.*, **11**, 319–326.

Hunter, J. R., Craig, P. D. and Phillips, H. E. (1993) On the use of random walk models with spatially variable diffusivity. *J. Comput. Phys.*, **106**, 366–376.

Kiørboe, T., Saiz, E. and Visser, A. W. (1999) Hydrodynamic signal perception in the copepod *Acartia tonsa*. *Mar. Ecol. Prog Ser.*, **179**, 97–111.

Klymak, J. M. and Gregg, M. C. (2001) The three-dimensional nature of flow near a sill. *J. Geophys. Res.*, **106**, 22295–22311.

Klymak, J. M. and Gregg, M. C. (2003) The role of upstream waves and a downstream density-pool in the growth of lee-waves: stratified flow over the Knight Inlet sill. *J. Phys. Oceanogr.*, **33**, 1446–1461.

Klymak, J. M. and Gregg, M. C. (2004) Tidally generated turbulence over the Knight Inlet sill. *J. Phys. Oceanogr.*, **34**, 1135–1151.

Kunze, E., Dower, J. F., Beveridge, I. *et al.* (2006) Observations of biologically generated turbulence in a coastal inlet. *Science*, **313**, 1768–1770.

Lentz, S. J. (1992) The surface boundary layer in coastal upwelling regions. *J. Phys. Oceanogr.*, **22**, 1517–1539.

Mackas, D. L., Denman, K. L. and Abbott, M. K. (1985) Plankton patchiness: biology in the physical vernacular. *Bull. Mar. Sci.*, **37**, 652–674.

Mackas, D. L., Kieser, R., Saunders, M. *et al.* (1997) Aggregation of euphausiids and Pacific Hake (*Merluccius productus*) along the outer continental shelf off Vancouver Island. *Can. J. Fish. Aquat. Sci.*, **54**, 2080–2096.

Mackas, D. L., Sefton, H., Miller, C. B. *et al.* (1993) Vertical habitat partitioning by large calanoid copepods in the oceanic subarctic Pacific during spring. *Prog. Oceanogr.*, **32**, 259–294.

Mackenzie, B. R., Miller, T. J., Cyr, S. *et al.* (1994) Evidence for a dome-shaped relationship between turbulence and larval fish ingestion rates. *Limnol. Oceanogr.*, **39**, 1790–1799.

Mauchline, J. (1980) The biology of Mysids and Euphausiids. In Blaxter, J. H. S., Russell, F. S. and Yonge, M. (eds), *Advances in Marine Biology*. Vol. 18. Academic Press, London, UK, 681 pp.

O'Brien, J. J. (1970) A note on the vertical structure of the eddy exchange coefficient in the planetary boundary layer. *J. Atmos. Sci.*, **27**, 1213–1215.

Ohman, M. D. (1990) The demographic benefits of diel vertical migration by zooplankton. *Ecol. Monogr.*, **60**, 257–281.

Onsrud, M. S. R., Kaartvedt, S., Rostad, A. *et al.* (2004) Vertical distribution and feeding patterns in fish foraging on the krill *Meganyctiphanes norvegica*. *ICES J. Mar. Sci.*, **61**, 1278–1290.

Patria, M. P. and Wiese, K. (2004) Swimming in formation in krill (Euphausiacea), a hypothesis: dynamics of the flow field, properties of antennular sensor systems and a sensory–motor link. *J. Plankton Res.*, **26**, 1315–1325.

Perlin, A., Moum, J. N., Klymak, J. M. *et al.* (2005) A modified law-of-the-wall applied to oceanic bottom boundary layers. *J. Geophys. Res.*, **110**, (C10S10). doi:10.1029/2004JC002310.

Press, W. H., Teukolsky, S. A., Vettering, W. T. *et al.* (1992) *Numerical Recipes in C: the art of scientific computing*. Cambridge University Press, New York, USA, 994 pp.

Ross, T., Gaboury, I. and Lueck, R. (2007) Simultaneous acoustic observations of turbulence and zooplankton in the ocean. *Deep Sea Res. I*, **54**, 143–153, doi:10.1016/j.dsr.2006.09.009.

Ross, T. and Lueck, R. (2003) Sound scattering for oceanic turbulence. *Geophys. Res. Lett.*, **30**, 1343, doi:10.1029/2002GL016733.

Rothschild, B. J. and Osborn, T. R. (1988) Small-scale turbulence and plankton contact rates. *J. Plankton Res.*, **10**, 465–474.

Rubjakov, X. (1970) The possible causes of diel vertical migrations of planktonic animals. *Mar. Biol.*, **6**, 98–105.

Sameoto, D. D., Jaroszynski, L. O. and Fraser, W. B. (1980) BIONESS, a new design in multiple net zooplankton samplers. *Can. J. Fish. Aquat. Sci.*, **37**, 722–724.

Simard, Y., de Ladurantaye, R. and Therriault, J.-C. (1986) Aggregation of euphausiids along a coastal shelf in an upwelling environment. *Mar. Ecol. Prog Ser.*, **32**, 203–215.

Simard, Y. and Lavoie, D. (1999) The rich krill aggregation of the Saguenay - St. Lawrence Marine Park: hydroacoustic and geostatistical biomass estimates, structure, variability, and significance for whales. *Can. J. Fish. Aquat. Sci.*, **56**, 1182–1197.

Simard, Y. and Mackas, D. L. (1989) Mesoscale aggregations of euphausiid sound scattering layers on the continental shelf of Vancouver Island. *Can. J. Fish. Aquat. Sci.*, **46**, 1238–1249.

Stanton, T. K. and Chu, D. (2000) Review and recommendations for the modelling of acoustic scattering by fluid-like elongated zooplankton: euphausiids and copepods. *ICES J. Mar. Sci.*, **57**, 793–807.

Strickler, J. R. (1982) Calanoid copepods, feeding currents and the role of gravity. *Science*, **218**, 158–160.

Stull, R. B. (1988) *Introduction to Boundary Layer Meteorology*. Kluwer Academic Publication, 666 pp.

Thomson, D. J. (1984) Random-walk modeling of diffusion in inhomogeneous turbulence. *Q. J. Roy. Met. Soc.*, **110**, 1107–1120.

Thomson, R. E. and Allen, S. E. (2000) Time series acoustic observations of macrozooplank- ton diel migration and associated pelagic fish abundance. *Can. J. Fish. Aquat. Sci.*, **57**, 1919–1931.

Trevorrow, M., Mackas, D. and Benfield, M. (2005) Comparison of multi-frequency acoustic and in situ measurements of zooplankton abundances in Knight Inlet, BC. *J. Acoust. Soc. Am.*, **117**, 3574–3588.

Tsurumi, M., Mackas, D. L., Whitney, F. A. *et al.* (2005) Pteropods, eddies, carbon flux, and the climate variability in the Alaska Gyre. *Deep Sea Res. II*, **52**, 1037–1053.

Tunnicliffe, V. and Syvistsky, J. P. M. (1983) Coral move boulders: an unusual mechanism of sediment transport, Knight Inlet, British Columbia. *Limnol. Oceanog*, **28**, 564–586.

Verity, P. G. and Smetacek, V. (1996) Organism life cycles, predation, and the structure of marine pelagic ecosystems. *Mar. Ecol. Prog Ser.*, **130**, 227–293.

Visser, A. W. (1997) Using random walk models to simulate the vertical distribution of particles in a turbulent water column. *Mar. Ecol. Prog Ser.*, **158**, 275–281.

Widder, E. A. and Frank, T. A. (2001) The speed of an isolume: a shrimp's eye view. *Mar. Biol.*, **138**, 669–677.

Yamazaki, H., Mackas, D. L. and Denman, K. L. (2003) Coupling small-scale physical processes with biology. In Robinson, A. R., McCarthy, J. J. and Rothschild, B. J. (eds), *The Sea*, vol. 12, pp. 51–112.

Yen, J., Rasberry, K. D. and Webster, D. R. (2008) Quantifying copepod kinematics in a laboratory turbulence apparatus. *J. Mar. Syst.*, **69**, 283–294.

APPENDIX: 1: ACOUSTIC DATA PROCESSING

The raw echo-sounder data were averaged vertically into 0.95 m depth bins, and horizontally by 4 pings (4 s or about 12 m in horizontal distance at a speed of 6 knots). These data were first converted to volumetric backscatter strength and the standard corrections made (Trevorrow *et al.*, 2005). The calibration data required for the corrections were collected while the ship was anchored in Hoeya Sound (beside the sill, 50°42.00′N, 125°58.00′W, Fig. 1A) and are estimated to be accurate to ± 0.8 dB, or a relative error of 20%. In our data, the observed backscatter within the scattering layer varied by a factor of roughly 2–10, while outside of this layer the backscatter was 3–4 orders of magnitude less.

The BIONESS and 38 kHz acoustic data indicated that the mid-depth (90 m) sound scattering layer near the sill was strongly dominated by *Euphausia pacifica* (Trevorrow *et al.*, 2005). The size and age distribution of these *E. pacifica* was unimodal, dominated by young adults born the previous spring. Elsewhere in the inlet there were times and places where most of the biomass in the deep scattering layer was made up of other zooplankters, such as siphonophores or large copepods, and fish (Trevorrow *et al.*, 2005). Scattering in the upper layer near the sill is caused primarily by physical microstructure (Ross and Lueck, 2003). Thus, *in situ* abundances were estimated by dividing the volumetric backscatter cross-section estimates by the population-averaged backscatter cross-section for an individual euphausiid at each of the echo-sounder frequencies.

The population averaged acoustic scattering model from Stanton and Chu (Stanton and Chu, 2000) was the most appropriate to our study (Trevorrow *et al.*, 2005). Euphausiids are represented by bent fluid cylinders. Distributions of their length and orientation are explicitly averaged within the model. We used the BIONESS data to determine the distribution of cylinder dimensions; length $= (15.9 \pm 1.3)$ mm (mean, standard deviation) with a length to radius ratio of 15 (M. Galbraith, unpublished data). We assume that the radius of curvature of the cylinders is $3\times$ the body length and that their orientation is horizontal $(0°) \pm 30°$ (mean, standard deviation). The sound speed and density contrast ratios (zooplankter vs. seawater) were assumed to be 1.025 and 1.045 (following Foote *et al.*, 1990). Thus, the model predicts average backscatter target strengths per animal of -97.8, -83.1 and -78.9 dB (re $1\ m^2$) for 38, 120 and 200 kHz, respectively. Abundances predicted by the model were quantitatively verified with simultaneous BIONESS trawls (Trevorrow *et al.*, 2005).

APPENDIX 2: MODEL PARAMETERS AND DATA METRICS

All parameters and symbols used are listed in Table IV.

Table IV: Model parameters and data metrics defined with units

Physical model parameters		
$\mathcal{D}$	–	Eddy viscosity
h_0	m	Average water column depth upstream of sill, constant
h_b	m	Water column depth over sill, variable
h_{min}	m	Water column depth at top of sill, constant
k_m	$m^2\ s^{-1}$	Eddy viscosity in interior flow
κ	–	Von Karman constant
L_1	m	Horizontal location of beginning of sill slope
L_2	m	Horizontal location of top of sill
Δt	s	Time step in model
U	$m\ s^{-1}$	Mean flow velocity upstream of sill, constant
u	$m\ s^{-1}$	General mean horizontal velocity
u_a	$m\ s^{-1}$	Horizontal velocity in the mean flow over sill, variable
u_a	$m\ s^{-1}$	Friction velocity
w_m	$m\ s^{-1}$	Mean vertical velocity
x	m	General horizontal coordinate
z	m	General vertical coordinate
z_b	m	Thickness of bottom boundary layer (bbl)
z_{sl}	m	Thickness of 'surface' layer, bottom of bbl
Zooplankton behaviour parameters		
w_{zoo}	$m\ s^{-1}$	Vertical component of zooplankter swim velocity
z_i	m	Preferred light depth of zooplankter
z_{tol}	m	Zooplankter's "acceptable" distance away from z_i
zoo_{basic}	$m\ s^{-1}$	Comfortable zooplankter swimming speed
zoo_{max}	$m\ s^{-1}$	Maximum zooplankter swimming speed
Data metrics		
φ	rad	Phase of tide
CF	–	Concentration factor
C_i	$\#\ m^{-3}$	Concentration of animals approaching the sill
FI	m	Flow index
t_a	h	Time aggregation was sampled relative to previous slack tide
VI	m	Velocity index
ΔZ	m	Displacement depth of aggregation below Z_i
Z_i	m	Preferred light depth of animals approaching the sill

APPENDIX 3: PHYSICAL MODEL

Topography

The model replicates the main features of the topography on each side of the sill. In general, there is a deep plain, followed by a linear slope and a shallow plain (Fig. 3A). On the east (landward) side, the bottom depth, h_b, is given by

$$h_{bE}(x) = \begin{cases} h_0 & x < L_1 \\ h_0 - (h_0 - h_{min})\dfrac{x - L_1}{L_2 - L_1} & L_1 < x < L_2 \\ h_{min} & x > L_2 \end{cases} \quad (3)$$

where $h_{min} = 60$ m, $h_0 = 200$ m, $L_1 = 1000$ m, $L_2 = 3250$ m and x is the horizontal location increasing as the sill is approached (Fig. 3A). On the west (seaward) side, the slope has two sections and is steeper, especially near the top of the sill (Fig. 1B). The basin is not quite as deep. The bottom depth is given by

$$h_{bW}(x) = \begin{cases} h_0 & x < L_1 \\ h_0 - (h_0 - h_1)\dfrac{x - L_1}{L_b - L_1} & L_1 < x < L_b \\ h_1 - (h_1 - h_{min})\dfrac{x - L_b}{L_2 - L_b} & L_b < x < L_2 \\ h_{min} & x > L_2 \end{cases} \quad (4)$$

where again $h_{min} = 60$ m, while $h_0 = 150$ m, $h_1 = 130$ m, $L_1 = 2000$ m, $L_b = 2500$ m and $L_2 = 2880$ m.

Mean flow field

The mean flow is based on the Cummins (Cummins, 2000) model. It is steady and conserves volume as it passes over the slope. The horizontal velocity u_a in the model above the bottom layer (Fig. 3A) is:

$$u_a(x) = U\frac{h_0}{h_b(x)} \quad (5)$$

where $U = 0.18$ m s^{-1} is flow speed approaching the sill on the east side, and is about 10% higher on the west side (because the water column on the west side is shallower, so the same volume of water flows more quickly).

Friction velocity, u_*, is a measure of the surface stress. It is based on the velocity and eddy viscosity ($k_m = 0.01$ m^2 s^{-1}) above the bbl (bottom 10 m, shaded Fig. 3A) in the mean flow (Cummins, 2000) so that $u_* = (k_m u_a(x)/z_b)^{1/2}$. The flow velocity, $u(x, z)$, in the surface layer (bottom 10% of bbl) was assumed to vary linearly with depth (Fig. 3B) for simplicity (using a conventional log layer makes no difference to the zooplankton advection/aggregation patterns);

$$u(x,z) = u_*(x)\frac{z + h_b(x)}{z_{sl}}, \quad z < -h_b(x) + z_{sl} \quad (6)$$

where z is the vertical coordinate measured upward from the air–sea interface (so that z is always negative in the ocean). Above the surface layer in the bbl, the flow is quadratic and the velocities at the boundaries of adjacent layers are continuous.

$$u(x,z) = u_a(x) - (u_a(x) - u_*(x))\left(\frac{h_b(x) - z_b + z}{z_b - z_{sl}}\right)^2, \quad -h_b(x) + z_{sl} < z < -h_b(x) + z_b \quad (7)$$

and above the bbl

$$u(x,z) = u_a(x), \quad -h_b(x) + z_b < z \quad (8)$$

The mean vertical velocity w_m, set by conservation of mass, is:

$$w_m(x,z) = \begin{cases} 0 & x < L_1, x > L_2 \\ -u(x,z)\dfrac{h_0 - h_{min}}{L_2 - L_1}\dfrac{z}{h_b(x)} & L_1 < x < L_2 \end{cases}$$

Turbulent flow

In the free flow, the eddy viscosity is taken as a constant.

$$\mathcal{D} = k_m, \quad -h_b + z_b < z \quad (10)$$

The eddy viscosity in the bbl was modelled using the O'Brien (O'Brien, 1970) formulation:

$$\mathcal{D} = k_m + \left(\frac{-h_b + z_b - z}{z_b - z_{sl}}\right)^2 \left(\kappa u_* z_{sl} - k_m + \left(h_b - z_{sl} + z\right)\left(\kappa u_* + 2\frac{\kappa u_* z_{sl} - k_m}{z_b - z_{sl}}\right)\right), \quad -h_b + z_s l < z < -H_b + z_b \quad (11)$$

where κ is the dimensionless von Karman constant (0.4). In the surface layer, the eddy viscosity is given as:

$$\mathcal{D} = \kappa u_*(z + h_b), z < -h_b + z_{sl} \quad (12)$$

The maximum turbulent velocity shear occurs at about

40% of the depth of the bbl. The random walk is defined as a vertical step and a horizontal step of a random number (R, mean 0 and variance 1) multiplied by $(2\mathcal{D}\Delta t)^{1/2}$. In the bbl, the random walk must be corrected because of the non-constant diffusivity (Hunter *et al.*, 1993; Visser, 1997). Thus, the turbulent velocity was taken as

$$\left(1-\frac{R^2}{2}\right)\mathcal{D}'+R\left[\frac{2\mathcal{D}}{\Delta t}\right]^{1/2} \tag{13}$$

where $\mathcal{D}'$ is the derivative of the diffusivity in the vertical or horizontal direction for the vertical or horizontal step, respectively. Using an adaptive step-size can be an issue for non-uniform diffusivity (Brickman and Smith, 2002) but was not found to be here. This formulation for the turbulent velocities for the Runge–Kutta scheme maintained an initially well-mixed particle field (as required—see Thomson, 1984). The coefficient on the derivative of diffusivity is, on average, half that needed for a simple Euler scheme (Visser, 1997).